Influence of Structural and Topological Constraints on the Crystallization and Melting Behavior of Polymers. 1. Ethylene/1-Octene Copolymers†

A. Alizadeh, L. Richardson, J. Xu, S. McCartney, and H. Marand*

Departments of Chemistry and Materials Science and Engineering, Virginia Polytechnic Institute and State University, Blacksburg, Virginia 24061-0212

Y. W. Cheung and S. Chum

Polyolefin Research, The Dow Chemical Company, Freeport, Texas 77541

Received April 29, 1999; Revised Manuscript Received June 23, 1999

ABSTRACT: Studies of the crystallization, melting, and morphology of random ethylene/1-octene copolymers by a combination of differential scanning calorimetry and atomic force microscopy are presented. Two different crystallization mechanisms prevalent in separate temperature ranges are inferred from the effect of cooling rate on the temperature dependence of crystallinity, from the reversibility of crystallization/melting phenomena at the lowest temperatures, and from the temperature dependence of kinetic parameters describing isothermal crystallization and melting. Morphological studies of these copolymers demonstrate the coexistence of two distinct crystalline superstructures (i.e., lamellae and fringed-micellar or chain cluster structures) which we tentatively associate with the two crystallization mechanisms. The multiple melting behavior of these copolymers is associated with the existence of separate morphological entities and is not explained by a mechanism of melting−recrystallization−remelting. Finally, the upward shift of the melting endotherm of secondary crystals (i.e., these formed by the low-temperature mechanism) with longer crystallization times is explained by a decrease in the molar conformational entropy of the remaining amorphous fraction as a result of secondary crystallization.

Introduction

When polymers crystallize from the melt state, they do so only partially, leading to a morphology consisting of amorphous and crystalline domains. This violation of the Gibbs phase rule arises from the fact that the morphological features of crystallizable polymers are controlled by kinetic and not by thermodynamic factors. Through the pioneering work of Keller[1] and of his followers,[2] it appears well established that the chain-folded lamellar structure is the predominant morphological unit of homopolymers crystallized under quiescent conditions from the melt or solution. Lamellar structures are indeed observed for virtually all highly crystallizable polymers. Materials such as long-chain paraffins[3] and low molecular weight poly(ethylene oxide)[4] exhibit very high crystallinity and under appropriate conditions can form single crystals with large lateral dimensions and regular facetting. Extensive lateral crystal growth by a chain-folding process will only occur if the steric stresses that build up at the crystal basal plane can be sufficiently minimized during crystallization. Gambler's ruin type calculations[5] indicate that such stresses are kept to a minimum when the frequency of adjacent reentry folding is maximized. In low molecular weight flexible polymers the absence of significant entanglements and the much faster large-scale conformational rearrangements allow the chain-folding process to occur with more regularity (i.e., leading to significant tight adjacent reentry).[6]

We note, however, that an increase in intrinsic chain rigidity, chain length, or concentration of chemical, regio, or stereo defects along the polymer backbone leads to a lower degree of crystallinity and to the formation of lamellae with reduced lateral dimensions and poorer facetting. These observations are satisfactorily explained by the reduced ability for chains to execute frequent tight adjacent reentry folding during lamellar growth and the resulting increase in steric stresses at the crystal basal planes and in the number of crystallizable sequences that become trapped between lamellae. Whereas the variation in the degree of crystallinity with chain length and stiffness can be solely accounted for by kinetic effects associated with chain folding, the morphological evolution associated with the increase in chemical, regio, or stereo defects is thermodynamically controlled by the energetics of defect inclusion in the crystal phase. When defects can be included in the crystal phase, the morphological features are primarily controlled by the kinetics of chain-folded lamellar growth and the partitioning of defects between crystal and amorphous phases. On the other hand, when defects are totally excluded from the crystal lattice, one should expect, as proposed by Flory[7] on the basis of thermodynamic arguments, that the degree of crystallinity will be controlled at a given temperature by the crystallizable sequence length distribution. However, even in this case there is overwhelming evidence that kinetic effects are still considerable especially during crystallization of the longest sequences by a chain-folding lamellar growth process (see Discussion section). We note also that in many low-crystallinity polymers, such as poly(vinyl chloride),[8] crystalline lamellae are not the predominant morphological unit, and the concept of fringed-micellar structures[9−11] is still being used, as can be anticipated from Flory's classic treatment.[7]

* To whom correspondence should be addressed.

† Presented at Meetings of the American Physical Society in Los Angeles (March 1998) and Atlanta (March 1999).

10.1021/ma990669u CCC: $18.00
Published on Web 09/03/1999

According to the Gibbs phase rule, the coexistence of at least two phases at any temperature below the equilibrium melting temperature of a homopolymer implies that these "phases" are not in thermodynamic equilibrium. The mere fact that the thickness of crystalline lamellae is always much lower than the chain contour length implies that chain-folded polymer crystals are metastable. Similarly, the existence of an amorphous fraction below the equilibrium melting temperature implies that this fraction is also metastable. A semicrystalline homopolymer is a system out of equilibrium in permanent evolution toward the fully crystalline state. Three simple models of morphological evolution have so far been considered in the literature to describe secondary crystallization. First, lamellar crystals of polymers that display a crystalline α relaxation[12] can thicken isothermally at temperatures above this relaxation.[13] Secondary crystallization has also often been described as involving the nucleation and growth of new lamellar structures, between lamellae or between stacks of lamellae formed during the previous (i.e., primary) crystallization process.[14−18] A third model considers that secondary crystallization can be associated with the increase in crystal perfection through the annihilation of defects within or at the interfaces of crystalline regions.[19]

Therefore, one of the most important questions before us is concerned with the understanding of the actual sequence of events that describe morphological evolution during the solidification process, especially during the secondary crystallization stage. More specifically, we are interested in understanding how local structural or topological constraints affect the primary crystallization process and control the extent and the crystallizability of the amorphous fraction remaining after primary crystallization.

In this paper, we investigate the case where the constraints are of structural origin and, more specifically, are associated with a random distribution of noncrystallizable comonomers (1-octene) along the chain of an otherwise crystallizable polymer (linear polyethylene). In subsequent papers, we will consider constraints arising from chain length, local chain stiffness, and regio or stereo defects. To probe the influence of octene "defect" content on the crystallization processes, we will study the evolution of the melting behavior after crystallization at different temperatures and for different times, using differential scanning calorimetry. A further motivation for the present studies originates from a recent suggestion that these homogeneous ethylene/1-octene copolymers exhibit a wealth of morphologies, ranging from lamellar structures at low octene content to fringed-micellar-like entities at the highest octene content (ca. 12 mol %).[20,21] To avoid any misconception of our intended use of the term fringed-micellar structure, we imply by this terminology an aggregate of chains exhibiting some level of crystallographic packing over restricted distances (ca. few nanometers) in directions parallel and normal to the chain axis. Should this dual morphology be confirmed, one may anticipate a systematic evolution in both the crystallization kinetics (i.e., crystallization mechanism) and the melting behavior (i.e., morphological characteristics) of these copolymers as a function of the octene content. The morphology of these copolymers is probed with atomic force microscopy.

Table 1. Molecular Characteristics of Ethylene/1-Octene Copolymers

sample	M_w (g mol^{-1})	M_w/M_n	mol % octene
EO-0.0	71 800	3.22	<0.01
EO-3.4	116 000	2.34	3.37
EO-4.6	88 700	2.72	4.63
EO-8.2	100 800	2.15	8.22
EO-12.3	119 700	2.04	12.3

The Results section of this paper is organized in four parts dealing with investigations of (I) the increase in crystallinity with temperature during cooling from the melt at different rates, (II) the decrease in crystallinity with temperature during immediate reheating of samples crystallized by cooling at constant rate, (III) the melting behavior after cooling and isothermal crystallization at various temperatures and for various times, and (IV) the morphology of ethylene/1-octene copolymers by atomic force microscopy. In the discussion section, we attempt to bring all these experimental results within one coherent and universal crystallization model. The proposed crystallization model differs from others in the literature, in that we redefine primary and secondary crystallization stages on the basis of whether crystallization occurs by a chain-folding lamellar growth process from an unconstrained melt.

Experimental Section

Materials. The ethylene/1-octene copolymers considered in the present study were synthesized at The Dow Chemical Co. using the INSITE technology.[22] The molecular characteristics of these materials were provided by Dow Chemical and are listed in Table 1. M_W and M_W/M_N are in all cases close to 100 000 g mol^{-1} and 2, respectively. The octene content, determined by NMR spectroscopy, varied from less than 0.01 to 12.3 mol %, (i.e., ca. 0−60 hexyl branches per 1000 backbone carbon atoms). The samples are identified with the initials EO (ethylene/1-octene) followed by a number corresponding to the octene comonomer content expressed in mole percent.

Films of various thicknesses were prepared by molding at 165 °C and 150 psig under a nitrogen atmosphere for 5 min and subsequent quenching into an ice−water bath.

Calorimetric Studies. The thermal behavior of these samples was investigated by differential scanning calorimetry using a Perkin-Elmer DSC-7 operated under nitrogen with a dry ice−2-propanol bath. To reduce differences among samples due to thermal lag, similar discoid samples of 150 ± 20 μm thickness and 3.5 ± 0.5 mg mass were employed. Melting endotherms and crystallization exotherms recorded at 10 °C/min were independent of sample mass in the range 0.8−4 mg. Heating and cooling scans were performed at different rates from 1 to 40 °C min^{-1}. Indium and tin standards were used to calibrate the temperature scale during isothermal and heating experiments, except in some cases (see below) where we were particularly interested in the influence of heating rate on the melting behavior. The temperature calibration during cooling was achieved using the isotropic-to-nematic phase transition of *p*-azoxyanisole (T_{I-N} = 136.0 °C). Calibration with a sapphire standard permitted the determination of absolute heat capacities.

An increase in heating rate leads not only to a shift in the peak melting temperature but also to a broadening of the melting endotherm. If one wishes to study the effect of heating rate on the melting behavior, it is imperative to correct heating traces for broadening due to heat transfer effects, especially at high heating rates. Gray's procedure[23] was used as a first approximation for this purpose. The onset melting temperature of an indium sample sandwiched between two layers of PE increases linearly with heating rate, the slope of which is higher than that for a pure indium sample. This slope reflects the intrinsic thermal lag of the instrument as well as that due to the low thermal conductivity of polymers. Typical values

for this slope for pure indium using a Perkin-Elmer DSC-7 range between 2.5 and 3.5 s, while for an indium-sandwiched sample (150 μm thick PE layers) the slope ranges from 7 to 10 s. The time constants reported here are in agreement with literature data.[24] In Gray's model[23] the evolution of heat absorption by a sample heated at constant rate is calculated from the thermal resistivity of the sample and the experimental heat flow measured in the DSC at that heating rate. The slope of the melting onset of the indium-sandwiched sample as a function of heating rate is a good estimate of the sample thermal resistivity. This model is only applicable for heating rates less than ca. 40 °C/min.

Morphological Studies. Morphological studies were carried out using a Digital Instrument Dimension 3000 atomic force microscope (AFM). The AFM was operated in tapping mode at room temperature using nanosensor TESP (tapping etched silicon probes) type single beam cantilevers. Images were collected in the phase mode. Samples were prepared by melt pressing thin films to a thickness of 50−100 μm at 160 °C, quenching to room temperature, and subsequently remelting the sample with a free surface. Samples with a free surface were crystallized from the melt by cooling at a constant rate of 1 °C/min and were kept at room temperature for 3 h prior to AFM examination. All melting steps were carried out under dry nitrogen gas.

Results

I. Increase in the Degree of Crystallinity during Cooling. The melt crystallization behavior of various ethylene/1-octene copolymers was studied at cooling rates from 2 to 40 °C/min. In all cases, the samples were kept at 160 °C for 2 min prior to cooling. Figure 1a−c shows the variation of heat capacity with temperature during cooling for EO-0.0, EO-3.4, and EO-12.3. The temperature scale was calibrated for each cooling rate using *p*-azoxyanisole. The heat capacity data for a linear polyethylene (LPE) melt from the ATHAS data bank[25] are also shown (dotted lines). The experimental $C_p(T)$ of EO copolymers coincides in the liquid state with published data[26,27] for linear PE. This result appears to hold not only for EO copolymers but also for other ethylene/α-olefin copolymers investigated in our laboratory, when the comonomer content is less than ca. 15 mol %. Similar conclusions were previously reached by Wunderlich et al.[26,27] and Mathot et al.[28]

As observed in previous studies,[21,28] the crystallization process of EO copolymers takes place over a very wide temperature range. Even at the lowest temperature reached during the cooling experiments (−20 °C), the crystallization of high octene content copolymers is far from complete. Upon cooling from the melt, the crystallization process is characterized by a sharp high-temperature exotherm, followed immediately by a broader exotherm extending to much lower temperatures. Both the absolute and relative magnitudes of the enthalpy of crystallization associated with the sharp exotherm decrease systematically with increasing octene content.

We note that the temperature at maximum crystallization rate, a characteristic feature of the sharp exothermic transition, is strongly cooling rate dependent and shifts toward lower values as the octene content is increased. In addition, the presence of even a small amount of octene comonomers results in a dramatic reduction in the degree of crystallinity at all temperatures (Figure 2). The assumptions made for these crystallinity estimations and the inherent limitations in accuracy are briefly discussed in the Appendix. Inspection of Figure 2 reveals that the degree of crystallinity of EO-0.0 increases only slightly below 70 °C. In

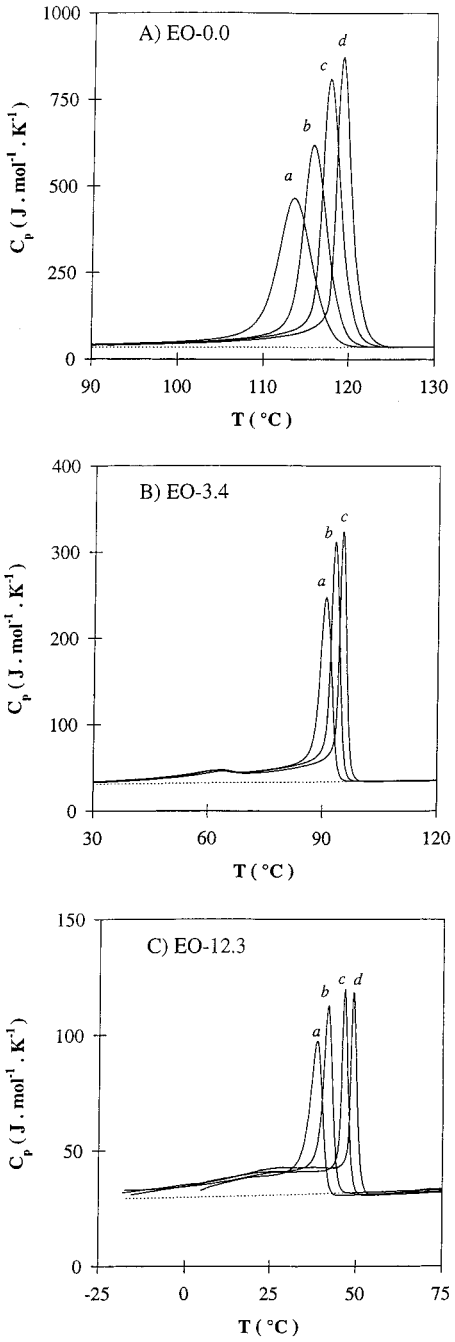

Figure 1. C_p vs T during cooling at various rates for (A) EO-0.0 (a, 40 °C/min; b, 20 °C/min; c, 10 °C/min; d, 5 °C/min), (B) EO-3.4 (a, 20 °C/min; b, 10 °C/min; c, 5 °C/min), and (C) EO-12.3 (a, 40 °C/min; b, 10 °C/min; c, 5 °C/min; d, 2 °C/min).

contrast, the degree of crystallinity of each copolymer exhibits a significant temperature dependence over a very large temperature range. Examination of Figure 2 and of similar data for other EO copolymers allows us to define a crossover temperature, T_R, below which the degree of crystallinity becomes cooling rate independent. T_R increases systematically with decrease in octene content.

The normalized degree of crystallinity (degree of crystallinity divided by the weight fraction of backbone ethylene sequences) reached upon cooling to −20 °C is plotted in Figure 3 as a function of comonomer mole fraction for EO copolymers. In this figure we have also included data from the literature on hydrogenated poly(butadiene) (HPB)[29,30] and data obtained in our labora-

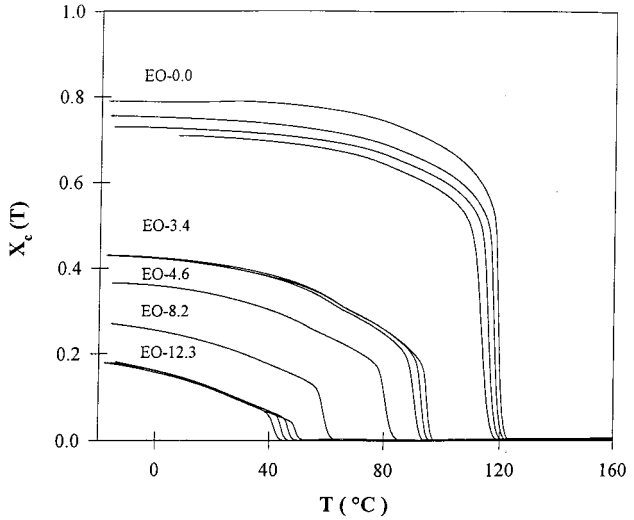

Figure 2. Degree of crystallinity as a function of temperature during cooling at different rates from the melt state for EO-0.0 (5, 10, 20, 40 °C/min), EO-3.4 (5, 10, 20 °C/min), EO-4.6 (20 °C/min), EO-8.2 (20 °C/min), and EO-12.3 (2, 5, 10, 40 °C/min).

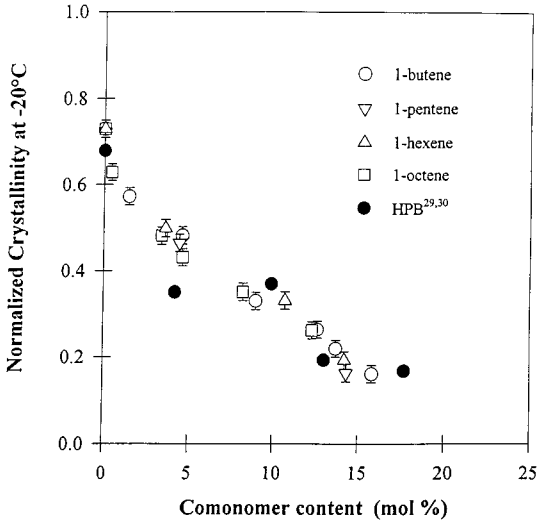

Figure 3. Normalized degree of crystallinity at −20 °C after cooling from the melt for ethylene/1-octene, ethylene/1-hexene, ethylene/1-pentene, and ethylene/1-butene copolymers. The normalized degree of crystallinity is obtained by dividing the actual degree of crystallinity by the weight fraction of ethylene sequences along the polymer backbone.

tory for other ethylene/α-olefin copolymers (1-butene, 1-pentene, and 1-hexene)[31] synthesized at The Dow Chemical Co. using the INSITE technology.[22] Since the calorimetrically determined degree of crystallinity is a weight-average quantity, we may expect that random copolymers exhibit the same degree of crystallinity only when they possess the same weight fraction of crystallizable sequences. At a given comonomer mole fraction, these ethylene/α-olefin copolymers exhibit different weight fraction of backbone ethylene sequences. Thus, to eliminate the a priori effect of branch size, we plot the normalized degree of crystallinity as a function of mole percent comonomer. Despite differences in the bulkiness of the branches (ethyl to hexyl), normalized crystallinity data for these different copolymers fall on the same curve. Since these materials have approximately the same chain length, the gradual decrease in degree of crystallinity with increase in comonomer content can be attributed to the increase in the concentration of ethylene sequences that are too short to crystallize.

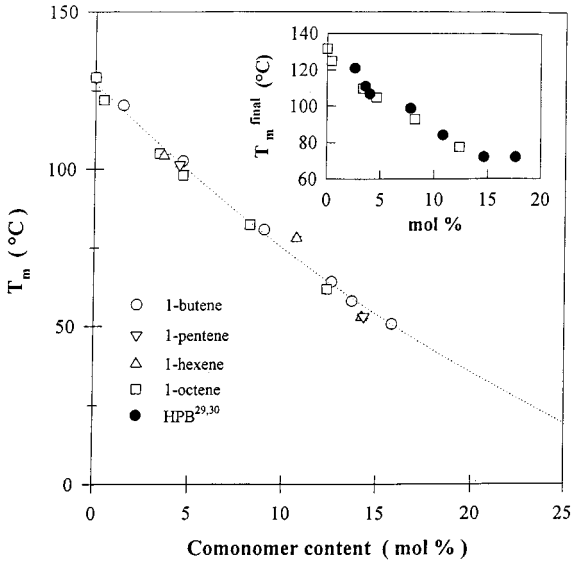

Figure 4. Peak melting temperature of ethylene/α-olefin copolymer as a function of the comonomer mole fraction. Insert shows the evolution of the final melting temperature for EO copolymers and hydrogenated poly(butadiene)s.[29,30]

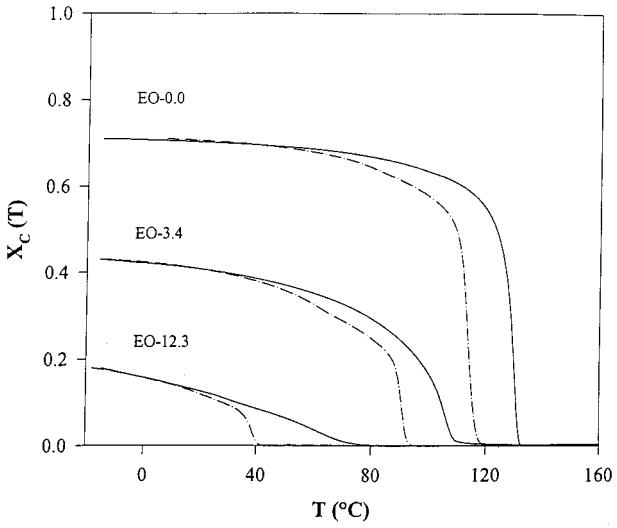

Figure 5. Degree of crystallinity during cooling from the melt at a rate of −40 °C/min (dashed curve) and subsequent heating at 10 °C/min (full curves) for EO-0.0, EO-3.4, and EO-12.3.

II. Decrease in the Degree of Crystallinity during Heating. We now report the results of heating experiments carried out immediately after cooling from the melt. The variation in peak melting temperature as a function of octene content is plotted in Figure 4. Also included are data obtained for other ethylene/α-olefin copolymers.[31] In all cases, peak melting temperatures correspond to specimens quenched rapidly from the melt to −20 °C (equivalent to a 40 °C/min cooling rate in a DSC-7). We note that different ethylene/α-olefin copolymers exhibit the same melting temperature for a given mole fraction of comonomers, regardless of the comonomer. In the in-box of Figure 4, we compare the final melting temperature of HPB's (where the last trace of melting is detected by calorimetry) reported by Crist et al.[30] with these of EO copolymers.

In Figure 5, we show the evolution of the degree of crystallinity during cooling from the melt to −20 °C and

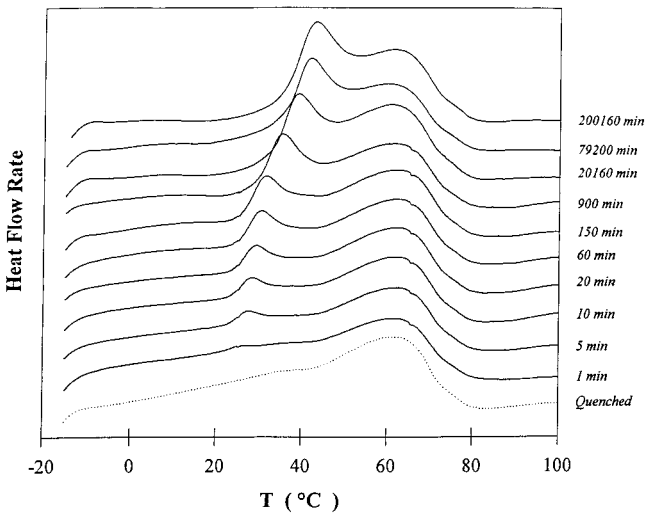

Figure 6. Evolution of the melting behavior for EO-12.3 after quenching from 160 to 20 °C, crystallization at 20 °C for various times from 1 min to 8 months, and subsequent quenching to −20 °C.

during immediate reheating, for linear polyethylene (EO-0.0) and for two copolymers EO-4.1 and EO-12.3. Significant differences in the behavior of linear polyethylene and EO copolymers become immediately apparent. EO-0.0 exhibits the expected hysteresis between crystallization and melting, and the largest change in crystallinity occurs at high temperature in the hysteretic loop. For statistical copolymers, the temperature dependence of the degree of crystallinity exhibits a hysteretic loop at high temperature and unambiguous reversibility in the low-temperature region. The increase in crystallinity during cooling becomes more significant for the low-temperature reversible process and less so in the high-temperature hysteretic region, when the octene content is raised. The onset temperature for the reversible crystallinity change decreases with increasing octene content and is identical with the crossover temperature, T_R, where the crystallinity becomes independent of cooling rate (Figure 2).

III. Melting Behavior after Cooling and Isothermal Crystallization. 1. Isothermal Crystallization at 20 °C. Copolymers of various octene content were quenched from 160 °C to 20 °C and held at this temperature for different periods of time. Figures 1 and 2 demonstrate that crystallization takes place during the cooling scan, leading to an initial degree of crystallinity at 20 °C which depends on comonomer content. After further crystallization at 20 °C for times ranging from 1 min to 8 months the samples were further quenched to −20 °C in the DSC and immediately reheated at a rate of 10 °C/min. The corresponding heating traces are shown in Figure 6 for EO-12.3. The melting trace of a sample heated after a direct quench from the melt to −20 °C is also shown for comparison (dotted curve). The melting curves of samples crystallized at 20 °C for various times reveal the presence of a "low endotherm" even for the shortest times. The development of this low endotherm is observed for all EO copolymers with ethylene content lower than 99.5 mol %. The low endotherm increases in magnitude and shifts toward higher temperatures for longer crystallization times. On the other hand, the location of the higher melting endotherm and the total heat of fusion, determined by integration from −20 °C to the end of

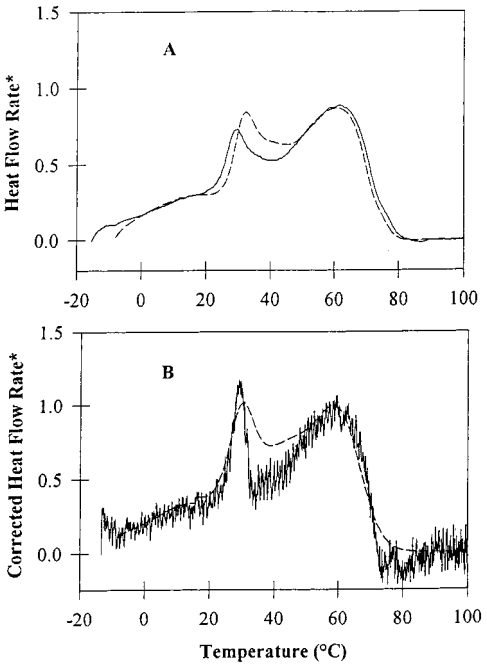

Figure 7. DSC heating traces of EO-12.3 after quenching from 160 to 20 °C, crystallization at 20 °C for 1 h, and subsequent quenching to −20 °C. Full and dashed curves for heating rates of 5 and 20 °C/min, respectively. (A) The temperature axis was corrected using the conventional metal standard calibration, and the ordinate was normalized for heating rates and masses. (B) The temperature axis was corrected using the sandwiched indium standard, and the ordinate was corrected using Gray's method. The scatter is a direct result of the use of Gray's method when the heating trace is recorded at low heating rate.

melting process, remain unaffected by the duration of the crystallization experiment.

Since EO copolymers crystallized under these conditions exhibit a multiple melting behavior, one may ask whether such behavior is explained by a mechanism of melting−recrystallization−remelting during heating.[21,28] To answer this question, we recorded heating traces of a given sample at different rates. In Figure 7a, heating traces are showed for EO-12.3 after crystallization at 20 °C for 60 min. In this figure the traces were recorded at 5 and 20 °C/min. The temperature axis was corrected using the conventional indium calibration at these rates. In Figure 7b, the heating traces are shown after correction using Gray's procedure[23] and calibration of the temperature scale with a sandwiched indium standard. We note that application of Gray's correction leads to the observation of a multiple melting behavior which is approximately independent of heating rate, thereby suggesting that there is no significant crystal reorganization during heating for these copolymers and for this range of heating rates.

Two different procedures are employed for analyses of the low endotherm enthalpy of fusion and melting temperature. In the first method, the DSC heating trace of the sample directly quenched to −20 °C was subtracted from that of samples crystallized at 20 °C. Figure 8 shows such curves obtained for EO-12.3 crystallized for different times. The subtracted curves display a negative deviation from zero with a minimum around the crystallization temperature followed by a positive deviation with a maximum between 5 and 20 °C above the minimum. This suggests that the increase in the low endotherm enthalpy of fusion is associated

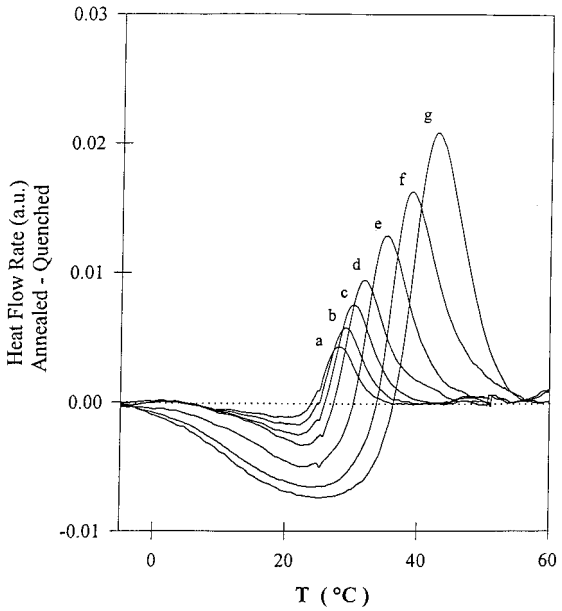

Figure 8. Evolution of the melting behavior of EO-12.3 after quenching from 160 to 20 °C, crystallization at 20 °C for various times from 1 min to 8 months, and subsequent quenching to −20 °C. The DSC heating trace for the quenched sample was subtracted from that of each the samples isothermally crystallized at 20 °C.

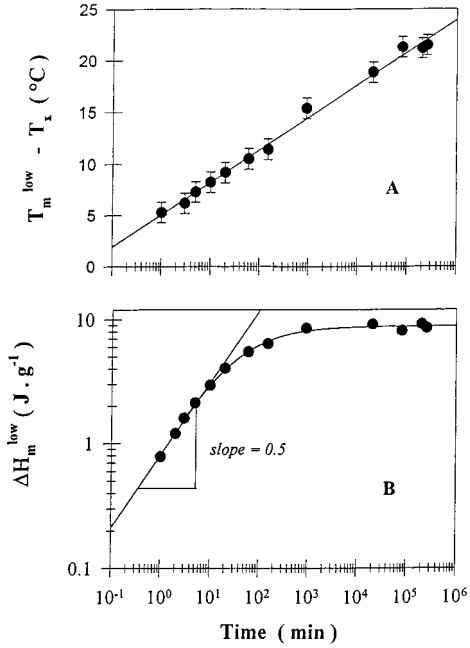

Figure 9. Evolution of the low endotherm characteristics for EO-12.3 after crystallization at 20 °C for different times: (A) low endotherm melting temperature; (B) low endotherm heat of fusion.

with an increase in the population of crystals formed at 20 °C from the amorphous fraction remaining after the quench from 160 to 20 °C. As the residence time at 20 °C is increased, a smaller number of amorphous sequences are available for crystallization during the subsequent quench from 20 to −20 °C. Therefore, a more negative contribution is observed in the subtracted DSC traces below 20 °C. Thus, we conclude that a larger fraction of the sequences, which given enough time could crystallize at 20 °C, do crystallize during cooling below 20 °C if the residence time at 20 °C is shortened. In the second method of analysis, the contribution of the low endotherm to the total heat of fusion was estimated through curve fitting and deconvolution processes. This procedure, which for the sake of brevity is not described here, gave within the experimental uncertainty identical results to the curve subtraction method. The low endotherm heat of fusion was then taken as the average of values obtained through integration of the Gaussian fit to the low endotherm and through integration of the heat flow rate either above or below the baseline in Figure 8. Support for the above analytical approach is obtained when considering the rather smooth variation of the low endotherm enthalpy of fusion and melting temperature as a function of log(t) shown in Figure 9a,b for EO-12.3 copolymer. We observe in Figure 9a that the relative position of the low endotherm ($T_m^{low} - T_x$, where T_x is the crystallization temperature) varies linearly with the logarithm of time over almost 6 decades. The dependence of the low endotherm T_m^{low} on log(t_x) can be expressed by

$$T_m^{low} - T_x = A(T_x) + B(T_x)\log(t_x) \qquad (1)$$

Identical results are observed for all other ethylene/1-octene copolymers investigated. Experimental values for A(20 °C) and B(20 °C) are collected in Table 2. Within experimental accuracy, it appears that these quantities do not depend on the octene content. The

Table 2. Parameters Describing the Evolution of the Low Endotherm after Crystallization at 20 °C

	T_m^{low} (eq 1)		X_c^{low} t_x < 60 min (eq 2)
sample	$A(T_x)$	$B(T_x)$	n
EO-0.0			
EO-3.4	5.5	2.87	0.50
EO-4.6	4.9	3.04	0.55
EO-8.2	4.9	3.01	0.55
EO-12.3	5.2	3.13	0.52

average slope, B(20 °C), is 3.0 ± 0.2. Furthermore, extrapolation of T_m^{low} to very short times yields in all cases the crystallization temperature, T_x (i.e., 20 °C). Similar results have been obtained for ethylene copolymers with other α-olefins,[31] for poly(arylene ether ether ketone),[33] bisphenol A polycarbonate,[34,35] poly(ethylene terephthalate),[36] and isotactic polystyrene.[37]

Figure 9b shows the temporal evolution of the low endotherm heat of fusion, ΔH_m^{low}. In keeping with Avrami analyses carried out under the free growth approximation,[38] a log−log representation is used. At the early stages log(ΔH_m^{low}) increases linearly with log(t_x) or

$$\Delta H_m^{low} = K t_x^{n} \qquad (2)$$

For short times and for all copolymers investigated, the slope, n, of log(ΔH_m^{low}) vs log(t_x) is equal to 0.50 ± 0.05. At times of 20−60 min and longer, a deviation from this power law is observed. In fact, ΔH_m^{low} is found to vary linearly with log(t_x) for times longer than 300 min. However, this further increase in crystallinity with time is so slow that ΔH_m^{low} appears, misleadingly so on a log−log plot, to reach a plateau characteristic of a given copolymer composition (Figure 9b). Our results indicate that the degree of crystallinity increases rapidly at short times and considerably more slowly although steadily at longer times.

We also investigated whether the cooling stage to −20 °C after crystallization at 20 °C had any effect on the

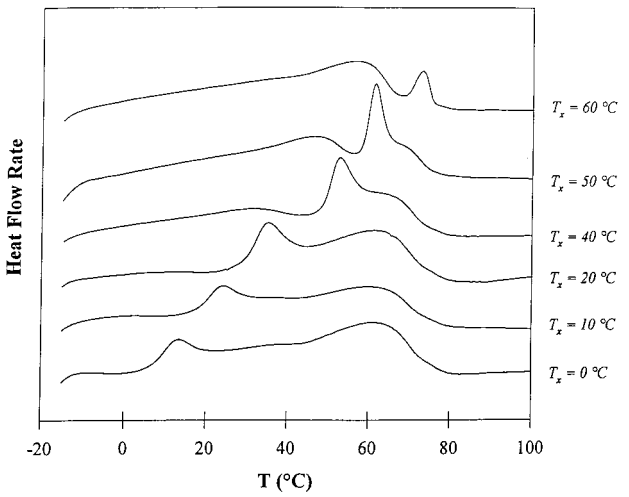

Figure 10. Heating traces for EO-12.3 crystallized for long times at temperatures between 0 and 60 °C and subsequently quenched to −20 °C.

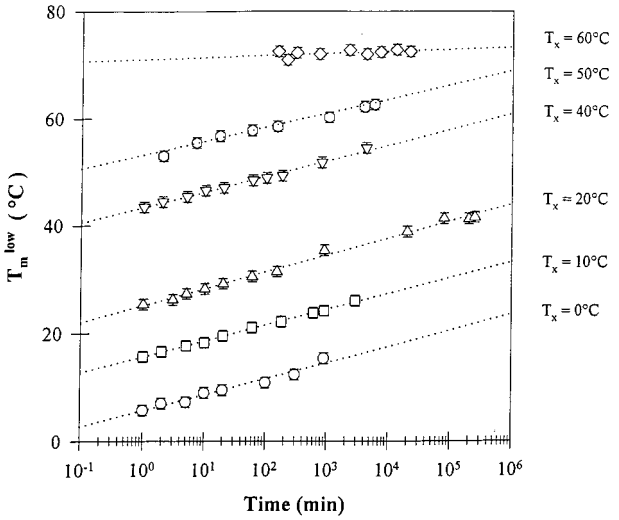

Figure 11. T_m^{low} vs log(t_x) for crystallization between 0 and 60 °C for EO-12.3.

low endotherm position and enthalpy of fusion. We found that baseline determination and data analyses were more easily carried out for samples cooled after isothermal crystallization but that the evolution of the low endotherm position and enthalpy of fusion with crystallization time were identical in both cases.

2. Influence of Temperature on Secondary Crystallization. The series of experiments presented here are very similar to those reported in the previous section, and the same methodology for the determination of the low endotherm melting temperature and heat of fusion has been used. The samples were quenched from the melt at 160 °C to the desired crystallization temperature, T_x, and maintained at that temperature for a given time, t_x. Then, the samples were further quenched to −20 °C, and their melting endotherm was immediately recorded at a rate of 10 °C/min.

A series of DSC thermograms of EO-12.3 isothermally crystallized at temperatures between 0 and 60 °C and subsequently cooled to −20 °C are shown in Figure 10. For this copolymer, crystallization at any temperature below 40 °C yields a series of melting traces that have similar characteristics to these shown for $T_x = 20$ °C in Figure 6: the occurrence of melting below the temperature where isothermal crystallization is carried out, a high endotherm which exhibits the same peak temperature and heat of fusion as the quenched sample, and finally a sharp endothermic transition just above the crystallization temperature. For crystallization temperatures above 40 °C, the sharp endothermic peak merges with the high endotherm, and substantial changes in the shape of the thermograms are observed (Figure 12). Most importantly, it is noted that for $T_x > 40$ °C crystallization proceeds isothermally in a sample totally devoid of initial crystallinity, while for $T_x < 40$ °C a certain fraction of the copolymer has already crystallized before reaching T_x, even at the highest cooling rates available experimentally (Figure 3). For $T_x \geq 50$ °C an induction time is required to detect the endothermic peak. This induction time grows rapidly as the crystallization temperature is raised. In contrast, for T_x below 50 °C the presence of a low endotherm is detected for crystallization times as short as 1 min.

Now, we focus on the time dependence of the low endotherm melting temperature after crystallization at different temperatures. We see in Figure 11 that in all

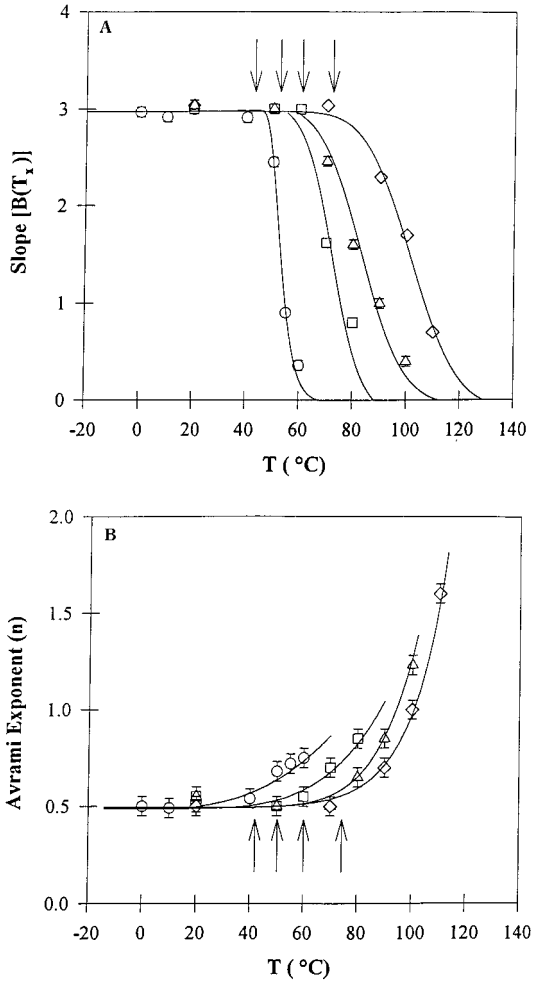

Figure 12. Crystallization temperature dependence of the low endotherm temporal evolution: (A) temperature dependence of $B(T_x)$, the slope of T_m^{low} vs log(t_x); (B) temperature dependence of n, the Avrami exponent.

cases T_m^{low} varies linearly with the logarithm of time. For $T_x < 50$ °C, T_m^{low} vs log(t_x) plots are parallel but shifted vertically, with slopes $B(T_x)$ (eq 1) close to 3 (see Table 3). Extrapolation of T_m^{low} to times of a few seconds consistently yields T_x, the crystallization temperature. However, a significant reduction of $B(T_x)$ is observed for $T_x > 50$ °C. The extrapolation of T_m^{low} to extremely short

Table 3. Parameters Describing the Evolution of the Low Endotherm after Crystallization at T_x for EO-12.3

	T_m^{low} (eq 1)		X_c^{low} t_x < 60 min (eq 2)
T_x (°C)	$A(T_x)$	$B(T_x)$	n
0	5.65	2.97	0.50
10	5.92	2.92	0.49
20	5.18	3.13	0.52
40	3.41	2.91	0.54
50	3.07	2.54	0.68
55	6.70	0.90	0.72
60	10.9	0.36	0.75

times results in a temperature that is considerably higher than the crystallization temperature, even after accounting for the induction period.

The analysis of the heat of fusion also reveals a discontinuity in the crystallization behavior at ca. 40−50 °C. The early stage of secondary crystallization is in all cases characterized by a linear variation of $\log(\Delta H_m^{low})$ with $\log(t_x)$, yet a significant change in the Avrami exponent is observed around 40 °C. While n is close to 0.5 for $T_x \leq 40$ °C, it increases continuously with temperature above 40 °C, reaching a value of 0.75 at 60 °C (Table 3).

Although the above behavior is characteristic of all EO copolymers investigated, the crossover temperature, T^*, where changes in the kinetic parameters n and B are observed, depends on comonomer content. Figure 12a illustrates the variation of $B(T_x)$ as a function of temperature for each copolymer. The temperatures T^*, where the change in slope ($B(T_x)$) occurs, are indicated by arrows for each copolymer. Similarly, Figure 12b shows the variation in the Avrami exponent, n, during the early stages of crystallization at various temperatures. The temperature where the Avrami exponent deviates from $^1/_2$ is in excellent agreement with the temperature where $B(T_x)$ becomes temperature-dependent. Additionally, we note that the value of n increases with decreasing octene content at the highest crystallization temperatures.

IV. Morphology. Some of the morphological features of EO copolymers obtained by AFM are shown in Figure 13a−d. As expected, EO-0.0 exhibits an ordered lamellar morphology. Although this morphology persists qualitatively in copolymers with lower octene contents (EO-3.4 and EO-8.2), the lamellae become considerably thinner and of smaller lateral dimensions (Figure 13b,c). Finally, the AFM picture for the highest branch content copolymer, EO-12.3, shows structures that resemble sheaves of very small dimensions, where individual lamellae are of such reduced dimensions that they are barely visible at this magnification. The aim of the above figures is to emphasize the continuous and dramatic change in morphology as the octene content increases. We note that AFM images of samples having the highest octene content were more difficult to obtain as these materials are more tacky.

The morphology of EO-4.6 is shown at higher magnification in Figure 14. Lamellar crystals organized in stacks are observed to coexist with interlamellar bridge-like structures. The interlamellar bridges appear to be oriented approximately normal to lamellar surfaces. We also note that the approximate dimensions (ca. few nanometers) of these interlamellar bridges are roughly the same as those of the granular structures reported in previous studies.[21] We will show in separate papers that similar morphologies are obtained with ethylene/1-butene copolymers[31] and ethylene/styrene interpolymers.[39]

AFM examination of high octene content copolymers crystallized under different conditions suggests that their morphology is cooling rate independent. Within the limits of the AFM resolution, the interlamellar bridges appear to exhibit the same dimensions regardless of the crystallization conditions. This observation must be contrasted with the observation in linear PE[14] and in conventional heterogeneous linear low-density polyethylene[40] that the lamellar morphology (i.e., the lamellar thickness and lateral dimensions, stack size) depends strongly on crystallization conditions. Similar observations have been previously reported on the basis of TEM studies of thin stained sections of various ethylene/α-olefin copolymers.[20,21,28,40] However, the existence of interlamellar bridges in these copolymers has, to our knowledge, not yet been reported in non-deformed materials quiescently crystallized from the pure melt state.

Discussion

A number of studies have addressed the melting behavior[30,41−45] of ethylene/α-olefin copolymers in the context of Flory's equilibrium theory[7] as well as some kinetic aspects of their crystallization process.[46] We know from Flory theory that in the case of A−B copolymers, where the comonomer B is totally excluded from the lattice of polymer A, the number of crystallizable sequences is continuously reduced as the crystallization temperature or the content in comonomer B increases. As ethylene/α-olefin copolymers are cooled from the melt, crystallization of ethylene sequences takes place in the order of decreasing sequence length. In previous studies, Alamo et al.[46] have addressed isothermal crystallization from the melt in a temperature range where only the longest ethylene sequences could crystallize. Here, we have extended such studies to copolymers of higher comonomer content and to lower temperatures, where shorter ethylene sequences are able to form crystals from a partially crystallized melt.

The discussion section is organized around three different themes so as to present a more coherent view of our findings. In the first part, we establish a link to previous studies and to Flory's theory by showing that the EO copolymers studied here conform to random statistics and that the octene comonomers are excluded from the polyethylene crystal lattice during quiescent crystallization. In the second section, we discuss a qualitative crystallization model for such copolymers, similar in nature to that recently proposed by Mathot et al.,[28] in which lamellar structures form from the longest ethylene sequences and fringed-micellar crystals or chain clusters form from shorter sequences. In this section, we also provide a number of experimental observations in support of this model and recall pertinent results from previous studies. In the third and last section, we show that the observed multiple melting behavior is not associated with a melting−recrystallization−remelting during heating; we provide a solid foundation to the concept of "low endotherm" and establish an unambiguous relationship between the low endotherm and the melting of secondary crystals in general. We then expand on the origin and universal characteristics of the crystallization time dependence of low endotherm.

I. Random Statistics and Comonomer Exclusion. Examination of Figures 3 and 4 shows that the compo-

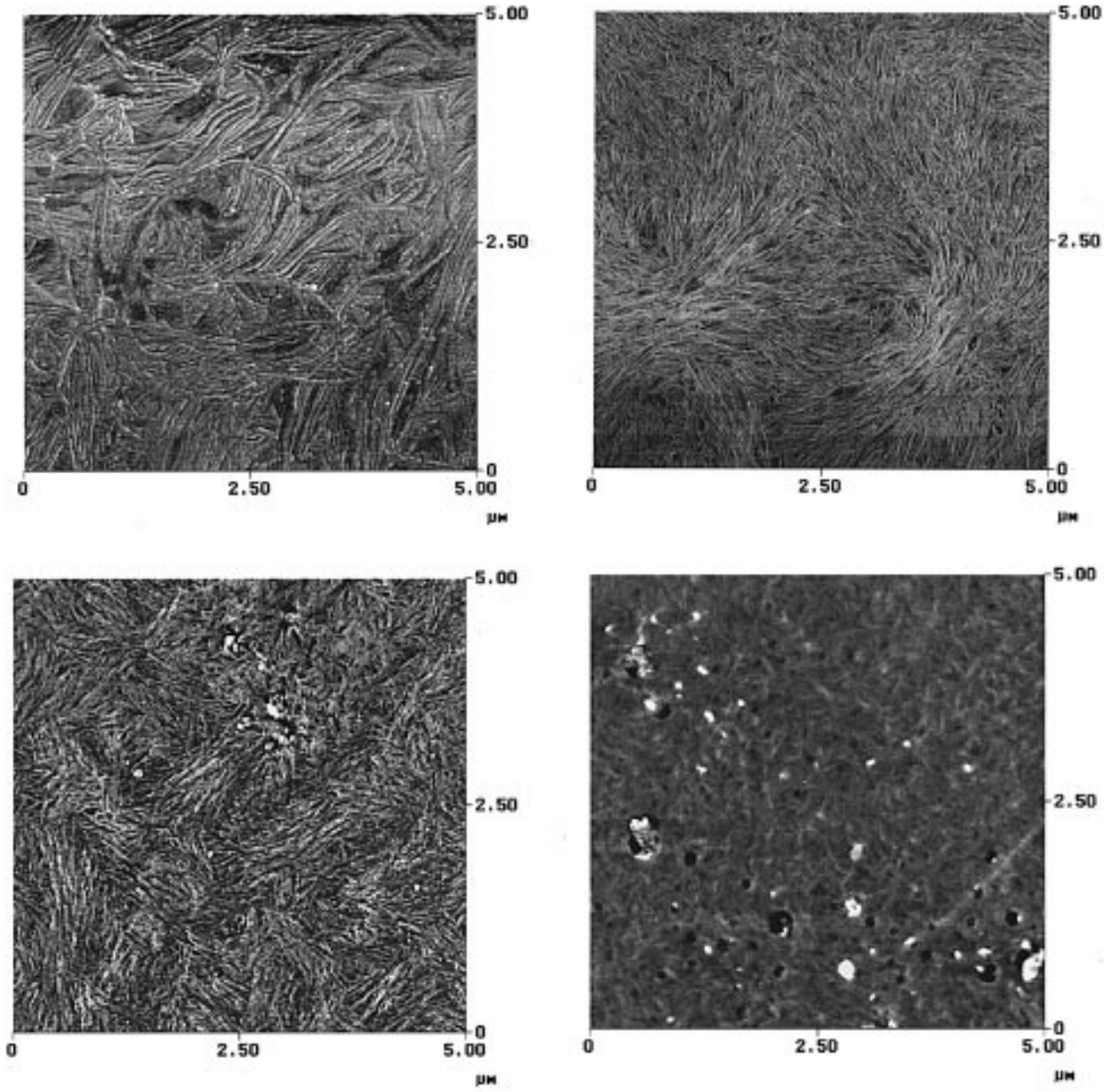

Figure 13. Atomic force micrographs in tapping mode (phase images) of (A) EO-0.0, (B) EO-3.4, (C) EO-8.1, and (D) EO-12.3 after crystallization during cooling from the melt at a rate of 1 °C/min.

sitional dependence of both the normalized degree of crystallinity and the melting temperature of ethylene/α-olefin copolymers prepared by the INSITE technology[22] is not sensitive to the nature of the comonomer and is identical to that reported for hydrogenated poly(butadienes).[29,30] Comonomer exclusion (branches larger than methyl), which is key for the use of Flory's treatment[7] of copolymer crystallization, has been previously established by a number of authors.[47−49] It is worth recalling that for a given pair of comonomers the melting temperature and degree of crystallinity do not depend on the copolymer composition per se but are controlled by the crystallizable sequence distribution and thus may be affected by the type of catalyst used for copolymerization.[28,41,42,50] We conclude then that the ethylene/α-olefin copolymers used in the present study have sequence distributions that are similar to model random copolymers (HPB's) and to materials thoroughly examined in previous reports[29−31,42−44] and that the above comonomers are predominantly, if not totally, excluded from the polyethylene lattice.

II. Crystallization Process. Flory's equilibrium model states that at a given temperature, T, only the fraction of ethylene sequences of length greater than some critical length, $\zeta^*(T)$, can participate in the crystallization process. As the crystallization temperature decreases, this critical length decreases. Assuming that the copolymerization process is random, the ethylene sequence distribution can be directly calculated from the binomial distribution. Knowledge of the sequence distribution then allows derivation of the equilibrium degree of crystallinity at a given temperature.[30] The observation that the experimentally determined degree of crystallinity is however invariably lower than the equilibrium prediction is consistent with the fact that polymer morphology is controlled by kinetic rather than by thermodynamic factors. Indeed, we know for fully crystallizable homopolymers that crystallization

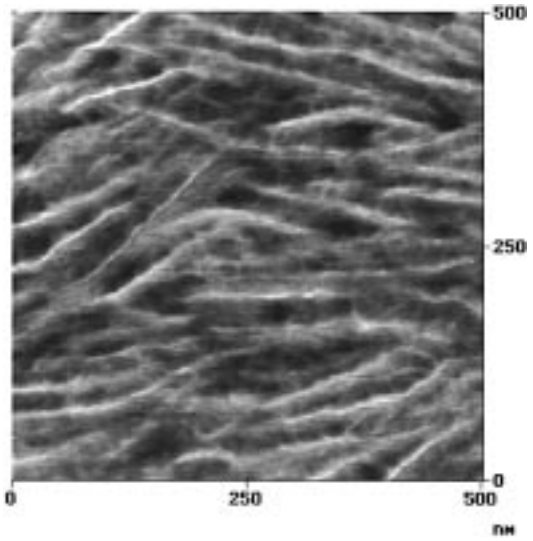

Figure 14. Atomic force micrographs in tapping mode of EO-3.4 after crystallization during cooling from the melt at a rate of 1 °C/min.

takes place at a measurable rate only well below the equilibrium melting temperature.[6] Previous studies of homopolymers also indicate that the thickness of the crystalline lamellae varies linearly with the reciprocal of the undercooling.[51,52] Simple thermodynamic arguments (Gibbs−Thomson) then lead to the well-verified prediction that fully crystallizable homopolymers cooled from the melt at higher rates (i.e., crystallized at lower temperatures) form lamellar structures that are thinner and, thus, melt at lower temperatures.[51,52] Previous studies have also shown for a number of polymers that even in the absence of thickening lamellar crystals melt substantially above their formation temperature;[53] i.e., the degree of crystallinity shows a significant hysteresis in consecutive cooling and heating cycles. Such hysteresis and the cooling/heating rate dependence of bulk crystallinity can then be viewed as the signature for a nucleation controlled process leading to chain-folded lamellar structures.[6,51]

As comonomers are randomly included along a polymer chain, the lamellar thickness is no longer strictly controlled by the undercooling but is mainly dependent on the crystallizable sequence distribution. While the longest sequences may still participate in the chain-folding lamellar growth process, the shortest sequences are excluded since branches are energetically prohibited to enter the crystal lattice. As a result of the complexity associated with chemical heterogeneity along the chain backbone, a kinetic model of crystal growth is yet to be given for such materials. While we cannot examine our experimental data in a more quantitative or theoretical context, some general remarks can be made. The lower the branch content, the larger the number of ethylene sequences that are long enough to undergo chain-folding and the larger the lateral dimensions and the perfection of lamellar crystals that can form at the lowest undercoolings. Upon further cooling, shorter ethylene sequences begin participating in the crystallization process. We note that the longest sequences of most chains may already be part of lamellar structures formed at higher temperatures. As initially pointed out by Richardson et al.,[45] the remaining sections of these chains are pinned at lamellar surfaces and are therefore topologically constrained. As these constraints become more significant, they prevent a number of shorter sequences to take part in further lamellar growth. However, these shorter sequences may be long enough to form stable clusters at sufficiently high undercooling, as one would envision during homogeneous primary nucleation. This latter mode of crystallization departs dramatically from a chain-folding lamellar growth process. First, considering a given copolymer chain, we anticipate that as the number of sequences involved in the crystallization process increases, the ability of remaining crystallizable sequences to undergo chain folding must decrease. The pinning of this chain at multiple locations should hamper the large conformational changes required during the reeling in process associated with the chain-folding mechanism. Such pinning would only allow local segmental motion, thereby only permitting aggregation between neighboring sequences of the same chain or of other chains. The extent to which these crystalline aggregates grow will be limited by the steric stresses that build at the crystal−melt interface in the absence of chain folding, by the concentration of crystallizable sequences in a given volume element, and by the ability of this sequences to diffuse, while pinned at one or two ends. The limited lateral growth of these crystals leads to high specific surface area and reduced stability. In other words, the melting temperature of such crystals would be much lower than that of a lamella of large lateral dimensions but the same thickness and may be just slightly above the crystal formation temperature. These crystals may therefore show no hysteretic behavior in cooling−heating cycles and appear to form and melt reversibly. As more and more of these crystals form, they would act as cross-link points effectively shifting the relaxation spectrum of the remaining amorphous fraction to higher temperature. The suggestion that these clusters of ethylene sequences or fringed-micellar structures act as cross-linking sites for the amorphous fraction will provide a new venue to address the time dependence of mechanical properties (physical aging) above the glass transition temperature.[54] The crystallization mechanism leading to such morphology should exhibit kinetic laws that differ from that associated with lamellar formation, leading to spherulitic or sheaflike superstructures. This qualitative model suggests that copolymer crystallization leads to lamellar structures at higher temperatures, where long sequences can undergo chain folding, and fringed-micellar or chain-cluster-like structures at the lowest temperatures, where chain folding of the shortest sequences is kept to a minimum or even nonexistent. Obviously, this is an oversimplification. The morphological transition from lamellar growth to fringed-micelle formation is gradual, where upon decreasing crystallization temperature or increasing branch content, lamellae become progressively thinner and of smaller lateral extent,[20,21,40] eventually resembling what some have referred to as mosaic blocks (loss of lattice coherence over extended length scales in direction normal to the chain axis) as a result of a decreasing tendency for adjacent reentry folding and associated increase in interfacial stresses. Finally, a stage may be reached where mostly nonfolded chain crystals of very small lateral dimensions, akin to primary nuclei, are formed. Obviously, there is no reason to a priori discard the possibility that long but isolated ethylene sequences that were not involved in lamellar formation at higher temperatures could take

part in chain cluster formation at lower temperature and display some level of chain folding.

We now provide support for this model on the basis of experimental results given in the previous section. Examination of Figure 1a−c supports the existence of two exothermic processes during cooling. The sharp exotherm shifts to lower temperature and decreases in magnitude as the octene content increases. The relative magnitude of the lower temperature exotherm increases with branch content. Examination of Figure 2 allows us to conclude that the high-temperature exotherm exhibits a strong cooling rate dependence, while the lower temperature exotherm occurs in the temperature range where crystallinity is independent of cooling rate. We also conclude that the fraction of the total degree of crystallinity, which is achieved in the low-temperature process, increases systematically with branch content.

We now turn to melting studies carried out immediately after cooling to −20 °C (Figure 5). Upon heating, the variation in degree of crystallinity with temperature tracks exactly that recorded during cooling only at the lowest temperatures, i.e., where the degree of crystallinity is observed to be cooling rate independent. At the highest temperatures, where the crystallinity varies with cooling rate, a hysteresis during cooling and heating cycles is observed. In agreement with the proposed model, two modes of crystallization are observed: at high temperature, cooling rate dependence and hysteresis for cooling/heating cycles are consistent with the classical nucleation-controlled chain-folded lamellar growth process, and at lower temperatures, cooling rate independence and reversible crystallization/melting processes are concordant with a mechanism leading to formation of crystallites of very small dimensions. Similar conclusions were very recently reported by Androsch et al.[55] on the basis of modulated DSC experiments. The temperature, T_R, where the transition in the crystallization mechanism is observed, decreases with increasing branch content. This result is explained by the slower lamellar growth expected from a reduced local concentration of sequences which are long enough to participate in the chain-folding process and by the increased frustration imposed on the crystallization of short sequences by that of the long ones. T_R should therefore depend on cooling rate and correspond to the temperature where crystallization is first observed during cooling. Isothermal treatment at any temperature below T_R leads to further crystallization in the presence of topological constraints.

To further support this dual crystallization mechanism, we now examine the results of crystallization studies carried above and below the crossover temperature T_R. We make the assumption that the low endotherm observed just above the crystallization temperature is associated with the melting of crystals formed during isothermal treatment. Although this assumption may appear trivial, the typical multiple melting behavior reported in this paper in Figures 6, 7, and 10 and by Androsch et al.[55] for EO copolymers and in the literature for a large number of polymers (PET, PEEK, etc.) is often explained by a mechanism of melting−recrystallization−remelting.[19,21,56] The demonstration that it is not so for EO copolymers is offered in the next section. Similar conclusions will be reported shortly for PEEK,[33] PET, and bisphenol A polycarbonate.[34,35] Under the stated assumption, study of the crystallization time dependence of the melting behavior provides a means to follow the evolution of the degree of crystallinity and crystal stability during isothermal crystallization. Results of these studies again point toward a dual crystallization mechanism. It is found that for each copolymer there exists a temperature T^*,[57] which increases with decreasing branch content, below which the Avrami exponent "n" is invariably equal to 0.5, and the low endotherm melting temperature is given by eq 1, where A and B are constant within experimental uncertainty and equal to 5K and 3K, respectively. Identical results were obtained in studies of other ethylene/α-olefin copolymers.[31] We note that an Avrami exponent of 0.5 has already been reported by Schultz et al.[58] for the secondary crystallization of linear polyethylene at temperatures below that of the primary crystallization. Such a value of the Avrami exponent was argued by these authors to be consistent with predictions for instantaneous nucleation and diffusion-controlled one-dimensional growth and possibly linked to the observation by Keith et al.[59] of intercrystalline links between edges of chain-folded lamellar crystals. One could however also interpret this Avrami exponent in the context of the fractal growth process discussed by Mathot et al.[28] Avrami exponents of value below 0.5 were reported recently by Fu et al.[60] for the secondary crystallization of ethylene/1-butene copolymers. We further note that the exponent of 0.5 is also observed during the early stage secondary crystallization of PEEK[33] and bisphenol A polycarbonate.[34,35]

The secondary crystallization mechanism proposed here differs from the lamellar insertion model discussed by Strobl and co-workers.[17] Indeed, we find it difficult to envision the crystallization of short ethylene sequences into lamellar structures because of the large steric stresses that are expected to develop in the absence of significant adjacent reentry folding. Accumulation of such stresses should lead to a reduction in the lateral crystal dimensions.

Above T^*, a systematic decrease in B and an increase in both A and n with crystallization temperature are observed for all copolymers. We note that an increase in the Avrami exponent n with decreasing branch content and increasing crystallization temperature is consistent with the development from the free melt of larger superstructures such as sheaves or spherulites, thus with the expectation of more perfect lamellar growth and better chain folding at lower branch content. The Avrami exponents reported here appear to be a little lower than these reported by Alamo et al.,[46] possibly a consequence of the higher molecular weight of our samples. It may also result from the fact that in our studies isothermal crystallization was carried out at higher temperatures (possibly due to a difference in the concentration of heterogeneities which control the primary nucleation rate). For each copolymer, the temperature T^* below which the kinetic parameters adopt temperature-independent values appears to correlate with the crossover temperature T_R below which reversibility sets in and cooling rate independence of the crystallinity is observed. In further support for the approximate equality between T^* and T_R, we note that below T^* extrapolation of the low endotherm peak melting temperature to short times (few seconds) yields the crystallization temperature (i.e., crystallization and melting processes appear to be reversible at short times), while above T^*, a marked difference between melting and crystallization temperatures persists even

after crystallization times are corrected for induction time effects. The reversibility of crystallization/melting processes during heating/cooling cycles below T^* further reinforces the suggestion made earlier that these crystals are not only thin but also of very small lateral dimensions. These various observations provide very strong support for our suggestion that a change in crystallization mechanism and resulting morphology occurs at $T^* = T_R$ for each copolymer. The temperature dependence of kinetic parameters (A, B, n) at temperatures above T^* is also consistent with our proposal that the degradation in the degree of perfection, lateral dimensions, and, probably, extent of adjacent reentry chain folding of lamellar structures is gradual and systematic as branch content is increased or crystallization temperature is lowered. Consideration of (1) the length of sequences that can crystallize at temperatures $T < T^*$ and (2) the limited dimensions of resulting crystals (see interlamellar structural features in AFM micrograph in Figure 14) leads us to speculate that chain folding and lateral growth may play only a very minor role in this low-temperature mode of crystallization.

III. Origin of the Low Endotherm and Its Crystallization Time Dependence. We now turn our attention to the nature of the low endotherm and the origin of its shift to higher temperatures with longer crystallization times. Studies of the effect of heating rate on the overall melting profile of EO copolymers (Figure 7) allow us to conclude that there is no apparent reorganization during heating at these rates and that the actual melting trace of such material is a direct reflection of the nature of the crystals present at the beginning of a DSC scan. Therefore, it is incorrect to explain the observed multiple melting behavior (see Figures 6, 7, and 10) in terms of a process of melting−recrystallization−remelting.

We now discuss the temporal evolution of the low endotherm ($T_x < T^*$). When flexible homopolymers such as polyethylene, poly(ethylene oxide), etc., are isothermally crystallized from the melt, the resulting melting temperature increases with crystallization time. This phenomenon is associated with the increased stability (decrease in crystal free energy) of lamellar crystals due to isothermal thickening. Evidence for the lamellar thickening mechanism has been obtained by small-angle X-ray scattering and Raman LAM studies.[61,62] The driving force for such a process is obviously a reduction of the specific surface of polymer crystals. As alluded to in the Introduction, whether or not lamellar thickening processes can take place is thought to depend on the availability of a mechanism for the motion of conformational defects within the crystal phase. We have also argued that isothermal thickening should only be observed in lamellar crystals of polymers that possess a crystal α relaxation.[12] However, we have previously suggested[63] that the existence of a crystal α relaxation is a necessary but not a sufficient condition for lamellar thickening. In the case of ethylene/α-olefin copolymers, large enough branches (ethyl and higher) likely to be at crystal−melt interfaces should significantly, if not totally, prohibit the lamellar thickening process. Such a conclusion is easily drawn from the observation that the upper melting temperature of EO copolymers depends only weakly on crystallization time.[64] A similar argument can be made for crystals melting at the low endotherm since their thickness along the c-axis is again thought to be controlled by the ethylene sequence length. One could also argue that their lateral dimensions increase with crystallization time, but such an explanation is not consistent with the intuitive idea that these dimensions are restricted by the buildup of interfacial stresses associated with a very low fraction of adjacent reentry folding (Gambler's ruin problem).[5] One could alternatively argue that an increase in crystal perfection is at the origin of the crystallization time dependence of the low endotherm temperature.

In marked contrast with these classical views of the crystallization time dependence of a melting transition, we propose that the shift of the low endotherm to higher temperatures is associated with the steady decrease in the conformational entropy of the remaining amorphous fraction as a result of secondary crystallization (fringed-micelle or cluster formation). This proposal is made on the basis of five observations. First, we recall some results obtained with poly(ether ether ketone),[33,37] poly(ethylene terephthalate),[36] and isotactic poly(styrene)[37] for which both the glass transition and low endotherm melting temperatures are observed to increase linearly with the logarithm of secondary crystallization time. In these systems, we established direct correlations between the rates at which the low endotherm and the glass transition shift to higher temperatures.[33,37,65] Second, we recall that the crystallization process at temperatures below T^* is akin to a cross-linking process, where fringed-micellar structures act as network junctions. Third, we recall that a low endotherm similar to these discussed here was observed for ultrahigh molecular weight polyethylene after crystallization at temperatures as low as −100 °C. As this temperature is significantly below the α_c relaxation isothermal thickening effects are not expected. Fourth, we note that any defect diffusion or lamellar thickening process is thermally activated and thus should exhibit higher rates at higher temperatures. The temperature dependence of B is inconsistent with such expectations. Finally, we show (see below) that the upward shift of the low endotherm peak temperature is not associated per se with a lowering of the crystal phase free energy and thus must be due to an increase in the amorphous fraction free energy. We speculate that the increase in melt free energy, compensated by the free energy reduction due to crystallization, is entropic in nature and associated with the increase in configurational constraints imposed on the remaining amorphous fraction as a result of fringed-micellar crystallization. To show that this effect is not associated with the absolute stability of the crystal phase per se, we carried out two-step crystallization studies at temperatures below T^* for EO-12.3. This copolymer was first quenched to 30 °C where it was crystallized for 30 min and was subsequently quenched to 10 °C where it was further crystallized for different times ranging from 0 to 720 min. Although some lamellae form during the quench to 30 °C, we know from the above investigation that at $T = 30$ °C $< T^*$ we form some secondary crystals of the fringed-micellar type. Subsequent cooling to 10 °C and isothermal hold at this temperature for different times leads to a new population of crystals also of the fringed-micellar type, but with shorter ethylene sequences. Melting of these samples after the second crystallization step leads to the DSC traces shown in Figure 15. Of the three observed endotherms, only that associated with the melting of crystals formed at 10 °C exhibits

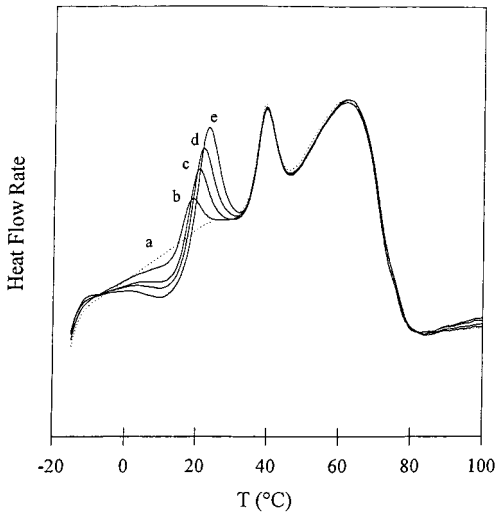

Figure 15. Heating traces at 10 °C/min of EO-12.3 cooled from 160 to 30 °C, annealed at 30 °C for 30 min, cooled to 10 °C, and subsequently annealed at 10 °C for various times: (a) 0 min, (b) 10 min, (c) 60 min, (d) 180 min, and (e) 720 min and finally cooled to −20 °C. All cooling steps were carried out at −40 °C/min.

dependence on the time of crystallization at 10 °C. The middle and upper endotherms are associated with the melting of crystals formed at 30 °C and during cooling from 160 to 30 °C, respectively. After crystallization at 10 °C for different times, there is not the slightest evidence for a shift of the upper two endotherms. Since one anticipates that an increase in crystal size or perfection is generally associated with a thermally activated defect diffusion process, one must conclude from the difference in behavior for the lower two endotherms that the observed behavior is not associated with any process occurring in the crystal phase. If, on the other hand, we assume that endothermic shifts are associated with the decrease in configurational entropy of the remaining amorphous fraction during secondary crystallization, then it is indeed expected that the melting point of the crystal population formed at the lowest temperature should increase with crystallization time. Indeed, for longer crystallization times, we expect a larger number of constraints on the amorphous fraction surrounding these crystals and thus lower molar conformational entropy for the remaining amorphous fraction. On the other hand, when we melt the population of crystals formed at or above 30 °C, samples that were crystallized for different times at 10 °C have lost complete memory of the isothermal step at 10 °C and therefore produce the same melting trace above the lowest endotherm. Similar observations are made when different temperatures are chosen for the two-step crystallization process. We note that similar experiments carried out with other semicrystalline polymers (i.e., PEEK, PET), which also exhibit the multiple melting behavior described here, lead to the same results.[33,37] The above arguments strongly suggest that the shift of the low endotherm toward higher temperature with longer crystallization time reflects a decrease in the conformational entropy of amorphous chains between crystallites. Related arguments were invoked by Wunderlich[27] for the discussion of the melting behavior of nonequilibrium crystals and their reduced entropy of fusion, especially in the case of fringed-micellar crystallites. These observations provide a new venue to explain the physical aging-like behavior of semicrystalline polymers above their glass transition.[54]

We conclude this section with a brief discussion of the use of SAXS technique for morphological studies of these semicrystalline polymers. Rather than attempting to reconcile the large amount of available SAXS data on linear and branched polyethylene crystallization[17,30] with our specific model, we draw the attention of the reader to a number of significant issues in the analysis of small-angle scattering. First, we recall that the reliability of any scattering analysis is always severely limited by the appropriateness of the model used to describe the morphology. In the present study, we not only showed that the lateral dimensions of lamellar structures and the extent of lamellar stacking decrease with increased octene content but we also demonstrated that the lamellar morphology coexists with fringed-micellar structures. The latter observation clearly indicates that the fluctuation in electron density along the normal to the lamellar surface is far from matching that expected for the idealized stacked plate model used in the classical analysis. One should therefore be extremely cautious when using this technique to gain a quantitative assessment of morphological evolution during crystallization.

Future studies should focus on the nature of secondary crystals since their formation and their influence on the remaining amorphous fraction are believed to be at the origin of the time dependence of the physical properties of semicrystalline polymers. A detailed analysis of such crystals will likely require an arsenal of experimental techniques. The studies presented in this paper suggest that secondary crystallization cannot be explained solely by secondary lamellar growth. The results of these studies lead us to favor a general mechanism, where secondary crystallization leads to fringed-micelle or chain cluster structures under conditions of high topological constraints, mosaic block crystals, when the constraints are reduced and secondary lamellae when the constraints are minimum.

Conclusions

Studies of the crystallization and melting behavior of EO copolymers suggest a dramatic change in mechanism and resulting morphology below a characteristic crystallization temperature T^*, which depends on composition. Crystallization below T^* leads to the formation of crystals of very small dimensions which for short crystallization times melt just above their formation temperature. The temperature T^* is associated with the crossover temperature, T_R, where the degree of crystallinity becomes independent of cooling rate. T^* can be further defined as the temperature at which ethylene sequences that are pinned at crystal surfaces start to participate in a more constrained crystallization process, leading to fringed-micellar or chain-cluster-like crystallites. The observation below T^* of an Avrami exponent equal to $^1/_2$ suggests the onset of a different crystallization mechanism below that temperature. We note that the same $^1/_2$ exponent has been obtained recently in our laboratory for as widely different polymers as ethylene/α-olefin copolymers (R > CH_3), bisphenol A polycarbonate, and poly(arylene ether ether ketone) and is likely to be universal for the secondary crystallization of chain sections that are topologically constrained. The crystallization time dependence of the melting temperature of secondary crystals is accounted for by the gradual decrease in the melt molar conformational entropy resulting from secondary crystalliza-

tion. Secondary crystallization can therefore be viewed as an efficient thermoreversible cross-linking phenomenon; thus, it is of significance for a better understanding of the time and temperature dependence of the physical properties of semicrystalline polymers above T_g. Crystallization of EO copolymers above T^* takes place from the free melt and leads to lamellar structures of increasing perfection and size for higher crystallization temperature or lower ethylene content. A gradual evolution toward linear PE behavior is observed for the parameters describing crystallization kinetics and crystal stability, as the crystallization temperature is raised above T^* and the octene content is decreased. Finally, we emphasize that the multiple melting behavior resulting from isothermal crystallization of EO copolymers is not associated with a melting−recrystallization−remelting process but with the melting of separate populations of crystals of different stabilities and formed from crystallizable sequences of different lengths.

Acknowledgment. We acknowledge support of this work by The Dow Chemical Co. Partial support from the National Science Foundation through a Young Investigator Award (DMR 93-57512) is also acknowledged. We also gratefully acknowledge the donation of a DSC-7 by the Perkin-Elmer Corp. Discussions of this work with Drs. F. Khoury, J. Schultz, B. Crist, M. Muthukumar, S. Z. D. Cheng, and A. Keller are gratefully acknowledged.

Appendix

In the present work we used the theoretical value of the heat of fusion of orthorhombic PE (288.4 J/g) for the calculation of the degree of crystallinity. The reported degrees of crystallinity are however not absolute for the following reasons: (1) WAXD profiles[55,67] and IR[67] and NMR[68] spectra for these copolymers suggest the coexistence of at least two different crystallographic phases (the orthorhombic and possibly the hexagonal phases). Our study[67] further showed the same systematic decrease in average crystal density with increase in branch content, as reported by Howard and Crist for hydrogenated poly(butadiene).[69] Then, one should expect the heat of fusion of orthorhombic crystals to be higher than that associated with the other crystallographic modifications. This issue deserves special attention in crystallinity estimations for copolymer samples melting at the lowest temperatures, where lattice dilation should be more significant and where a nonorthorhombic crystal phase appears. (2) A second oversimplification in our analysis is associated with the neglect of the temperature dependence of the theoretical heat of fusion. (3) The last and perhaps most important simplification in our crystallinity calculations arises from the neglect of surface enthalpic contributions,[70] ΔH_e, which should be significant for fringed-micellar crystals.

References and Notes

(1) Keller, A. *Philos. Mag.* **1957**, *2*, 1171.
(2) See for example: Bassett, D. C. In *Principles of Polymer Morphology*; Alden Press: Oxford, 1981. Khoury, F.; Passaglia, E. In *Treatise on Solid State Chemistry*; Hannay, N. B., Ed.; Plenum Press: New York, 1976; Vol. 3, Chapter 6.
(3) Ungar, G.; Zeng, X.; Brooke, G. M.; Mohammed, S. *Macromolecules* **1998**, *31*, 1875.
(4) Arlie, J. P.; Spegt, P.; Skoulios, A. *Die Makromol. Chem.* **1967**, *104*, 212. Kovacs, A. J.; Gonthier, A. *Kolloid Z. Z. Polym.* **1972**, *250*, 530.
(5) Guttman, C. M.; DiMarzio, E.; Hoffman, J. D. *Polymer* **1981**, *22*, 1466.
(6) Hoffman J. D.; Miller, R. L. *Polymer* **1997**, *38*, 3151.
(7) Flory, P. J. *Trans. Faraday Soc.* **1955**, *51*, 848.
(8) Gilbert, M. *J. Macromol. Sci., Rev. Macromol. Chem. Phys.* **1994**, *C34* (1), 77.
(9) Herrmann, K.; Gerngross, O.; Abitz, W. *Z. Phys. Chem.* **1930**, *10*, 371.
(10) Herrmann, K.; Gerngross, O. *Kautschuk* **1932**, *8*, 181.
(11) Bryant, W. M. D. *J. Polym. Sci.* **1947**, *2*, 547.
(12) Boyd, R. H. *Polymer* **1985**, *26*, 1123. Boyd, R. H. *Polymer* **1985**, *26*, 1123.
(13) Statton, W. O. *J. Appl. Phys.* **1961**, *32*, 2332.
(14) Bassett, D. C.; Hodge, A. M. *Proc. R. Soc. London* **1981**, *A377*, 61.
(15) Wang, W.; Schultz, J. M.; Hsiao, B. S. *J. Macromol. Sci.* **1998**, *B37* (5), 667.
(16) Cebe, P. *J. Mater. Sci.* **1988**, *23*, 3721.
(17) Strobl, G. R.; Engelke, T.; Meir, H.; Urban, G. *Colloid Polym. Sci.* **1982**, *260*, 39. Strobl, G. R. In *The Physics of Polymers*; Springer-Verlag: Berlin, 1996.
(18) Kruger, K.-N.; Zachmann, H. G. *Macromolecules* **1993**, *26*, 5202.
(19) Jonas, A. M.; Russell, T. P.; Yoon, D. Y. *Macromolecules* **1995**, *28*, 8491.
(20) Chum, S. P.; Kao, C. I.; Knight, G. W. *Plast. Eng.* **1995**, 21.
(21) Minick, J.; Moet, A.; Hiltner, A.; Baer, E.; Chum, S. P. *J. Appl. Polym. Sci.* **1995**, *58*, 1371.
(22) Lai, S. Y.; Knight, G. W. *ANTEC Proc.* **1993**, *51*, 1188. INSITE is a Trademark of The Dow Chemical Co.
(23) Gray, A. In *Analytical Chemistry*; Plenum Press: New York, 1976; Vol. 1.
(24) Berstein, V.; Ergov, V. M. In *Differential Scanning Calorimetry of Polymers. Physics, Chemistry, Analysis, Technology*; Ellis Horwood: Chichester, U.K., 1994.
(25) ATHAS data bank: http://funnelweb.utcc.utk.edu/∼athas/databank/intro.html.
(26) Wunderlich, B. In *Thermal Analysis*; Academic Press: San Diego, CA, 1990.
(27) Wunderlich, B. *Macromolecular Physics*; Academic Press: New York, 1980; Vol. 3.
(28) Mathot, V. B. F.; Scherrenberg, R. L.; Pijpers, T. F. J. *Polymer* **1998**, *39*, 4542. Mathot, V. B. F.; Scherrenberg, R. L.; Pijpers, T. F. J.; Engelen, Y. M. T. *New Trends Polyolefin Sci. Technol.* **1996**, 71.
(29) Krigas, T.; Carella, J.; Struglinski, M.; Crist, B.; Graessley, W. W.; Schilling, F. C. *J. Polym. Sci., Polym. Phys. Ed.* **1985**, *23*, 509.
(30) Crist, B.; Howard, P. R. *Macromolecules* **1999**, *32*, 3057.
(31) Subramaniam, C.; Alizadeh, A.; Marand, H., manuscript in preparation.
(32) Rim, P. B.; Runt J. P. *Macromolecules* **1983**, *24*, 258.
(33) Marand, H.; Alizadeh, A.; Desai, R.; Farmer, R.; Velikov, V.; Prabhu, V. *Macromolecules*, in press. *Bull. Am. Phys. Soc.* **1999**, *44* (1), 753.
(34) Alizadeh, A.; Quinn, J.; Sohn, S.; Richardson, L.; Marand, H., manuscript in preparation. *Bull. Am. Phys. Soc.* **1999**, *44* (1), 608.
(35) Sohn, S.; Alizadeh, A.; Marand, H., manuscript in preparation. *Bull. Am. Phys. Soc.* **1999**, *44* (1), 295.
(36) Marand, H.; Sholtz, P.; Verma, R.; Prabhu, V.; Vivirito, V. *Bull. Am. Phys. Soc.* **1996**, *41* (1), 450.
(37) Velikov, V. Ph.D. Dissertation, Virginia Polytechnic Institute and State University, 1996.
(38) Göler, V. F.; Sachs, G. *Z. Phys.* **1932**, *77*, 281.
(39) Alizadeh, A.; Xu, J.; Moreland, T. J.; Christian, S.; Marand, E.; Marand, H. *Bull. Am. Phys. Soc.* **1999**, *44* (1), 609. Manuscript in preparation.
(40) Voigt-Martin, I. G.; Alamo, R.; Mandelkern, L. *J. Polym. Sci., Polym. Phys.* **1986**, *24*, 1283.
(41) Alamo, R.; Domszy, R.; Mandelkern, L. *J. Phys. Chem.* **1984**, *88*, 6587.
(42) Alamo, R.; Mandelkern, L. *Macromolecules* **1989**, *22*, 1273.
(43) Alamo, R.; Mandelkern, L. *Thermochim. Acta* **1994**, *238*, 155.
(44) Crist, B.; Williams, D. N. *J. Macromol. Sci., Phys.*, in press.
(45) Richardson, M. J.; Flory, P. J.; Jackson, J. B. *Polymer* **1963**, *4*, 221.
(46) Alamo, R.; Mandelkern, L. *Macromolecules* **1991**, *24*, 6480.
(47) Laupretre, F.; Monnerie, L.; Barthelemy, L.; Wairon, J. P.; Sanzean, A.; Roussel, D. *Polym. Bull.* **1986**, *15*, 159.
(48) Perez, E.; VanderHart, D. L.; Crist, B.; Howard, P. R. *Macromolecules* **1987**, *20*, 78.
(49) Hay, J. N.; Zhou, X. Q. *Polymer* **1993**, *34*, 1002.

(50) Mathot, V. B. F.; Pijpers, M. F. *J. Appl. Polym. Sci.* **1990**, *39*, 979.
(51) Hoffman, J. D.; Davis, G. T.; Lauritzen, J. I. In *Treatise on Solid State Chemistry*; Hannay, N. B., Ed.; Plenum Press: New York, 1976; Vol. 3, Chapter 7.
(52) Barham, P. J.; Chivers, R. A.; Keller, A.; Martinez-Salazar, J.; Organ, S. J. *J. Mater. Sci.* **1985**, *20*, 1625.
(53) Marand, H.; Xu, J.; Srivatsan, S. *Macromolecules* **1998**, *31*, 8219.
(54) See for example: Struik, L. C. E. *Physical Aging of Amorphous Polymers and Other Materials*; Elsevier: Amsterdam, 1978. Struik, L. C. E. *Polymer* **1987**, *28*, 1521. However, note that this author assumes that the change in the physical properties of semicrystalline polymers above T_g is not a consequence of an increase in crystallinity and the associated increase in constraints in the amorphous fraction, but is a true physical aging of the rigid amorphous fraction.
(55) Androsch, R. *Polymer* **1999**, *40*, 2805. Androsch, R.; Blackwell, J.; Chvalun, S. N.; Wunderlich B. *Macromolecules* **1999**, *32*, 3735. Androsch, R.; Wunderlich, B. *Macromolecules*, submitted.
(56) Fougnies, C.; Damman, P.; Villers, D.; Dosiere, M.; Koch, M. H. J. *Macromolecules* **1997**, *30*, 1385. Fougnies, C.; Damman, P.; Dosiere, M.; Koch, M. H. J. *Macromolecules* **1997**, *30*, 1392.
(57) For the same reason that T_R depends on cooling rate, we should also expect T^* to increase with decreasing cooling rate. The lower the rate at which a sample is cooled, the higher the temperature where the first trace of crystallinity will be observed and the higher the upper crystallization temperature where the sample will still exhibit an Avrami exponent of $^1/_2$.
(58) Schultz, J. M.; Scott, R. D. *J. Polym. Sci. A-2* **1969**, *7*, 659.
(59) Keith, H. D.; Padden, F. J., Jr.; Vadimsky, R. G. *J. Appl. Phys.* **1971**, *42*, 4585.
(60) Fu, Q.; Chiu, F.-C.; McCreight, K.; Guo, M.; Tseng, W. W.; Cheng, S. Z. D.; Keating, M. Y.; Hsieh, E. T.; Deslauriers, P. J. *J. Macromol. Sci., Phys.* **1997**, *B36* (1), 41.
(61) Hoffman, J. D.; Weeks, J. J. *J. Chem. Phys.* **1965**, *42*, 4301.
(62) Duglosz, J.; Fraser, G. V.; Grubb, D.; Keller, A.; Odell, J. A.; Goggin, P. L. *Polymer* **1976**, *17*, 471.
(63) Xu, J.; Srinivas, S.; Marand, H.; Agarwal, P. *Macromolecules* **1998**, *31*, 8230.
(64) The magnitude of $B(T)$ decreases dramatically for $T > T^*$ and approaches zero at high temperatures (Figure 12a). The values obtained here are actually much lower than for linear polyethylenes (Stack, G. M.; Mandelkern, L.; Voigt-Martin, I. G. *Polym. Bull.* **1982**, *8*, 421).
(65) Marand, H.; Alizadeh, A. *Bull. Am. Phys. Soc.* **1999**, *41* (1), 1671.
(66) Sakaguchi, F.; Mandelkern, L.; Maxfield, J. *J. Polym. Sci., Polym. Phys. Ed.* **1976**, *14*, 2137.
(67) Alizadeh, A.; Subramaniam, C.; Christian, S.; Richardson, L.; Xu, J.; Marand, E.; McCartney, S.; Marand, H. *Bull. Am. Phys. Soc.* **1999**, *41* (1), 1562. Manuscript in preparation.
(68) Nieto, J.; van Heeringen, M. J. M. *Proc. Europ. Symp. Polym. Spectrosc.* **1994**, 52.
(69) Crist, B.; Howard, P. R. *J. Polym. Sci., Polym. Phys. Ed.* **1989**, *27*, 2269.
(70) Mandelkern, L.; Allou, A. L.; Golapan, M. *J. Phys. Chem.* **1968**, *72*, 309.

MA990669U